

# Online and Offline Determination of QT and PR Interval and QRS Duration in Electrocardiography

Martin Bachler<sup>1,2</sup>, Christopher Mayer<sup>2</sup>, Bernhard Hametner<sup>2</sup>,  
Siegfried Wassertheurer<sup>2</sup>, and Andreas Holzinger<sup>3</sup>

<sup>1</sup> Vienna University of Technology, Institute for Analysis and Scientific Computing,  
Wiedner Hauptstr. 8, 1040 Vienna, Austria

[Martin.Bachler@student.tuwien.ac.at](mailto:Martin.Bachler@student.tuwien.ac.at)

<sup>2</sup> AIT Austrian Institute of Technology, Health & Environment Department,  
Donau-City-Strasse 1, 1220 Vienna, Austria

<sup>3</sup> Institute of Medical Informatics, Statistics & Documentation,  
Medical University Graz, Auenbruggerplatz 2, A-8036 Graz, Austria

**Abstract.** Duration and dynamic changes of QT and PR intervals as well as QRS complexes of ECG measurements are well established parameters in monitoring and diagnosis of cardiac diseases. Since automated annotations show numerous advantages over manual methods, the aim was to develop an algorithm suitable for online (real time) and offline ECG analysis. In this work we present this algorithm, its verification and the development process.

The algorithm detects R peaks based on the amplitude, the first derivative and local statistic characteristics of the signal. Classification is performed to distinguish premature ventricular contractions from normal heartbeats. To improve the accuracy of the subsequent detection of QRS complexes, P and T waves, templates are built for each class of heartbeats.

Using a continuous integration system, the algorithm was automatically verified against PhysioNet databases and achieved a sensitivity of 98.2% and a positive predictive value of 98.7%, respectively.

**Keywords:** Electrocardiography, ECG, QRS complex, P wave, T wave, QT interval, PR interval, real time.

## 1 Introduction

Coronary heart diseases are the most common cause of death in Europe [1] and the second most in the United States, respectively [2]. In the diagnosis and monitoring of these diseases, electrocardiography (ECG) plays an important role. ECG measurements can be recorded fairly easily using skin electrodes on the chest or limbs and thus are widespread, non-invasive and painless [3].

The shape of one heartbeat in an ECG signal can be divided into a P wave representing the atrial depolarization, a QRS complex indicating the ventricular depolarization and a T wave displaying the ventricular repolarisation [4].

Segments and intervals between these features are well defined and established indicators in the diagnosis of cardiac diseases [4]. The most important of these intervals are [4]

- the PR interval, ranging from the beginning of the P wave to the beginning of the QRS complex,
- the QT interval, starting from the onset of the QRS complex to the offset of the T wave, and
- the duration of the QRS complex itself, ranging from the onset to the offset of the QRS complex.

Additionally, some non-antiarrhythmic drugs are found to cause an undesired prolongation of the QT interval. Therefore newly developed drugs are required to be assessed with respect to this effect [5]. The automation of the annotation of the ECG using signal analysis algorithms offers several advantages over manual methods. They are immune to observer related errors and operator fatigue, show higher accuracy in repeated measurements or allow for a faster or more extensive testing at lower cost.

A lot of ECG analysis methods have been developed in the last decades. Especially the rapid development of powerful computing hardware led to a widespread application of software ECG annotation algorithms in the last 30 years. Despite the usage of many different approaches such as signal derivatives [6], digital filters, wavelets and neural networks, most methods focus only on the detection of the QRS complex [7]. Other software algorithms combine existing QRS detectors with the evaluation of QT intervals [8,9] or P waves [10], but these methods are only suitable for offline ECG analysis. The challenge of correctly classifying biomedical signals is widespread and can be found, for example, in similar ways in the field of EEG analysis [11]. This paper presents an algorithm combining some of these methods and adopting them for online (real time) measurements.

## 2 Development Process

In this work we are addressing two fields of application of ECG annotation at the same time. One is the analysis of previously recorded signals using a common personal computer (offline) and the other one is the detection of features in the ECG in real time using an embedded system (online, real time). To avoid unnecessary complexity during the development process, we combined the work towards these goals as long as possible. Also, to relief the developer of repetitive tasks, we utilised the continuous integration system *Jenkins* [12,13]. Figure 1 shows the process of development split into its stages.

### 2.1 Offline Prototyping

The actual algorithm was developed and tested using the scientific computing environment MATLAB<sup>®</sup> as the first step of the process. MATLAB<sup>®</sup> allows easy matrix and vector manipulations, therefore it is perfectly suited for the

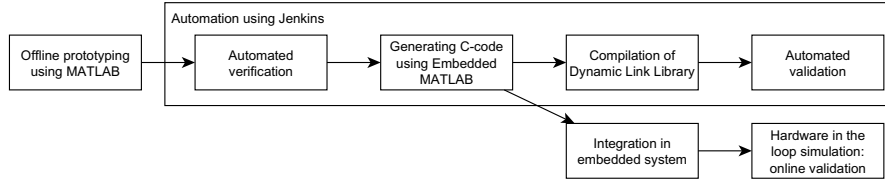


**Fig. 1.** Overview of the development process

rapid development of signal processing algorithms. Also, it can interface with other programming languages, including C, thus allowing an easy porting of the developed algorithm to digital signal processors in embedded systems or the compilation of dynamic link libraries (DLLs). Besides, MATLAB<sup>®</sup> allows the automation of the verification process using its scripting features, making it easy to integrate with continuous integration systems.

## 2.2 Continuous Integration Using Jenkins

Continuous integration tools help to implement “best practices” in software development by automating the whole building process (code generation, compilation, testing and verification) and the documentation thereof [14]. They mainly focus on the principles of centralisation, “test early, test often”, automation of build and documentation, and feedback. A continuous integration system usually features

- a version control repository,
- a continuous integration server,
- build scripts, and
- a feedback mechanism.

Version control repositories such as the *Concurrent Versions System* (CVS) or *Apache Subversion* (SVN) keep track of all changes made to the source files during development. The continuous integration system *Jenkins* monitors the CVS or the SVN and starts the building process as soon as a change in the source code is detected.

Automated software tests are performed by *Jenkins* after each successful build. Since developers are encouraged to commit changes in the source code after each single change, these changes are immediately integrated and tested by *Jenkins*. This approach narrows down bug tracking and facilitates to resolve errors [12,14].

## 2.3 Automated Verification

During the development process, the algorithm was continuously verified against ECG signals manually annotated by medical experts from different PhysioNet

databases [15,16] with respect to sensitivity, positive predictive value and the differences in time between features detected by the algorithm and annotations of the medical experts.

## 2.4 Generation of C-Code

After the successful verification of the algorithm, C-code was automatically generated from the MATLAB<sup>®</sup>-code. Since it allows efficient code generation, mainly to be used for embedded systems, but also suitable for ordinary PCs, Embedded MATLAB<sup>®</sup> was used for this task. It is a subset of the MATLAB<sup>®</sup> scientific computing language and can be easily automated using scripts. Therefore it was easy to integrate in *Jenkins* [12].

## 2.5 Compilation and Validation of PC Software

Using a standard C-compiler, a dynamic link library was built from the generated C-code by *Jenkins*.

In the next step, this library was validated using an established software testing environment. To ensure that the results are comparable, the same ECG signals that had been used for the verification were also used for validation. The library was considered to be valid only if the test reported no errors and if the results of verification and software tests matched completely.

## 2.6 Integration and Validation in the Embedded System

After all automated steps were carried out by the continuous integration system and verification and validation of the library were successfully finished, the C-code was manually integrated in an existing embedded system.

To validate this embedded system, a hardware-in-the-loop simulation was used. At this point, the embedded system was ready to use, but instead of measuring real ECG signals, they were simulated using a signal generator controlled by MATLAB<sup>®</sup>. In this simulation the signals previously used for verification were reproduced. This approach allows an efficient verification of the results as well as a validation of the final device.

## 3 Measurement Algorithm

R peaks are the most distinctive feature in ECG signals due to their high amplitude and steep slope. Therefore, they are easy to detect and can be used as a reference for other additional features. Thus, as shown in the overview in figure 2, the first step of the algorithm is to determine the R peaks as starting point for further signal analysis. The measurement algorithm detects R peaks in real time by continuously monitoring the amplitude and the first derivative of the signal [6]. Additionally, statistic characteristics of the signal are evaluated to prevent the algorithm from detecting motion artefacts as R peaks. After the

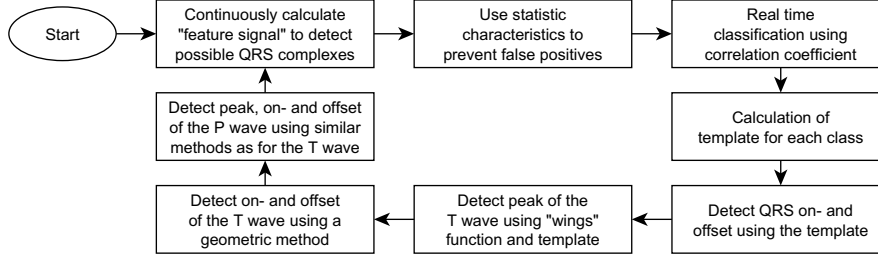


**Fig. 2.** Overview of the measurement algorithm

identification of an R peak a classification is performed to distinguish between premature ventricular contractions and normal QRS complexes. To reduce noise and enhance the accuracy of the detection of further features, templates are created by averaging each class of R peaks. The template's local amplitude is subsequently used to detect the QRS on- and offset. The peaks of T and P waves are found by analysing the signals first derivative [9]. Finally, the detection of the on- and offsets of T and P waves is based on a geometric method. These steps are described in more detail in the following subsections.

### 3.1 R Peak Detection

R peaks usually show a high signal amplitude, although sometimes the P wave can have an even higher amplitude. However, in contrast to the P wave, R peaks also show a steep slope of the signal. Therefore, R peaks can be detected by combining amplitude and first derivative of the signal and comparing them to a certain threshold.

To localise R peaks in the ECG tracing, a feature signal is continuously calculated as follows:

- Determine the first discrete derivative  $D_t$  of the signal  $S_t$

$$D_t = S_t - S_{t-1} . \quad (1)$$

- Calculate amplitudes  $SA_t$  of  $S_t$  and  $DA_t$  of  $D_t$  within a moving window ( $w = 60$  ms)

$$SA_t = \max(S_{(t-w)...t}) - \min(S_{(t-w)...t}) \quad (2)$$

$$DA_t = \max(D_{(t-w)...t}) - \min(D_{(t-w)...t}) . \quad (3)$$

- Derive  $C_t$  as a combination of  $SA_t$  and  $DA_t$

$$C_t = SA_t^2 \cdot DA_t . \quad (4)$$

- Calculate feature signal  $FS_t$  within a moving window ( $w = 100$  ms)

$$FS_t = \max(C_{(t-w)...t}) . \quad (5)$$

- Use the mean value of the last 2 seconds of  $FS_t$  as threshold  $Th_t$  ( $w = 2$  s)

$$Th_t = \frac{1}{w} \cdot \sum_{k=t-w}^t FS_k. \quad (6)$$

- Continue with the signal analysis only if

$$FS_t > Th_t. \quad (7)$$

Figure 3 shows different ECG signals with noise, small artefacts, high T waves and motion artefacts with their corresponding feature signals. The feature signal is robust regarding noise, small artefacts and prominent T waves, but does not respond to sudden motion of the subject.

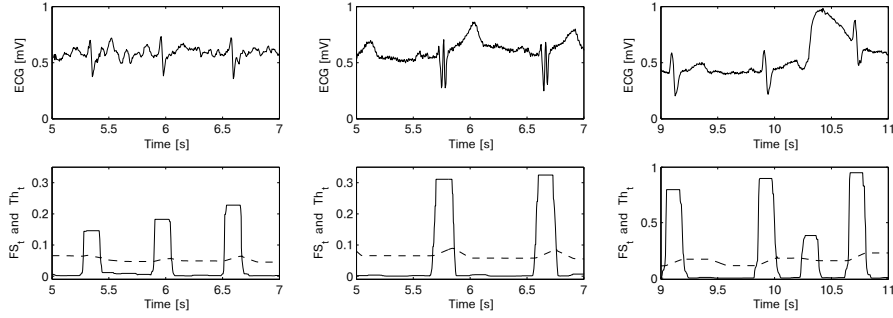


**Fig. 3.** Differently shaped ECG signals (top) and the response of feature signal  $FS_t$  (equation 5, bottom, solid line) and threshold  $Th_t$  (equation 6, dashed line)

Whenever the condition in equation 7 is fulfilled, the following statistic parameters are calculated. If these criteria are not reached, the evaluated part of the signal is considered as an artefact:

- Standard deviation  $\sigma$  within the last 400 ms

$$FS_t > Th_t + 6 \cdot \sigma^3. \quad (8)$$

- Kurtosis  $\beta_2$  within the last 2.5 seconds

$$\beta_2 > 4. \quad (9)$$

To find the R peak within each region of the QRS complex, local minima and maxima are calculated. The exact position of the R peak is chosen at the maximum with the biggest difference to its surrounding minima.

After the detection of more than two R peaks, a template is built by averaging them (see figure 4 (b) for an example). The correlation of the newly detected R

peak with the template is calculated to measure the similarity. If the correlation is below a certain threshold, the R peak is discarded.

To avoid false negative detections, the RR interval (interval between two consecutive R peaks) is calculated. If it exceeds 1.8 times the previous RR interval, this intermediate section is searched again, but with lower thresholds.

Subsequently, a real time classification of the R peaks is performed. The tracing of the last detected heartbeat is correlated with a predefined number of classes and is assigned to the class with the highest correlation. In the case that classes correlate better among each other than with the last detected heartbeat, these two classes are merged and a new class is created from the current heartbeat. Thus, in the real time version of the algorithm, classes evolve dynamically over time, continuously enhancing with the duration of the measurement. Figure 4 (a) shows the result of the classification of an ECG signal with pulsus bigeminus, a cardiovascular phenomenon where every second heartbeat is caused by a premature ventricular contraction [17]. The figure shows a complete separation of these two classes of heartbeats.

Furthermore, templates are created by averaging each class to reduce noise. Figure 4 (b) shows the template of a particularly noisy signal. As the level of noise exceeds the amplitude of the P wave, it would be impossible to detect this feature without the template. Therefore, the templates are used to detect all subsequent features (QRS on- and offset, P and T wave as well as their on- and offsets).

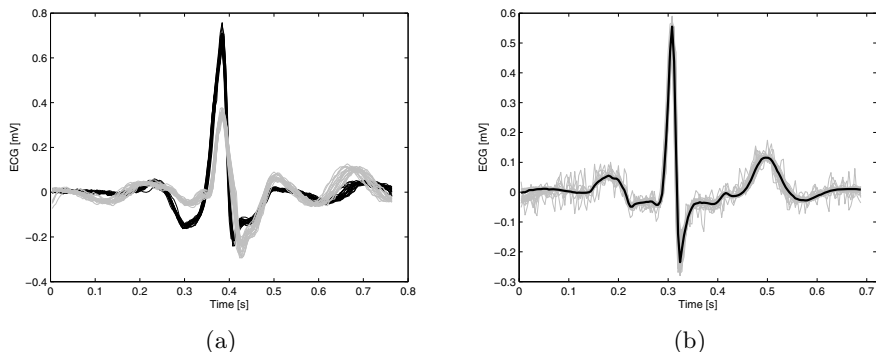


**Fig. 4.** (a) Result of the real-time classification of an ECG signal with pulsus bigeminus (every second heartbeat is a premature ventricular contraction [17]). (b) Template (black) of several heartbeats (grey) in a noisy signal.

### 3.2 On- and Offset of the QRS Complex

The onset of the QRS complex is the the point preceding the R peak, where the signal's slope is flat and its amplitude approaches the baseline. Similarly, the offset shows the same qualities after the R peak. Therefore, amplitude and first derivative of the signal are suitable measures to determine these points.

An interval of 150 ms right before the R peak is analysed to detect the onset of the QRS complex. This analysis is performed using the template as follows:

- Calculate the amplitudes  $TA_t$  and  $TDA_t$  of the template  $T_t$  and its first discrete derivative within a moving window ( $w = 30$  ms)

$$TA_t = \max(T_{(t-w)...t}) - \min(T_{(t-w)...t}) \quad (10)$$

$$TDA_t = \max(T'_{(t-w)...t}) - \min(T'_{(t-w)...t}), \text{ whereas} \quad (11)$$

$$T'_t = T_t - T_{t-1}. \quad (12)$$

- Calculate a threshold  $TT$  and  $TD$  for the amplitudes  $TA_t$  and  $TDA_t$

$$TT = c_1 \cdot (\max(TA_t) - \min(TA_t)) + \min(TA_t) \quad (13)$$

$$TD = c_2 \cdot (\max(TDA_t) - \min(TDA_t)) + \min(TDA_t) \quad (14)$$

with  $c_1$  and  $c_2$  being predefined constants.

- The point closest to the R peak, where  $TA_t$  is below  $TT$  or  $TDA_t$  is below  $TD$ , is annotated as the QRS onset.

The QRS offset is detected in the same way as the QRS onset, with two exceptions:

- The QRS complex might be pathologically prolonged, therefore a larger interval is chosen to be the analysed.
- In equation 10 and 11, window  $w$  is 60 ms.

### 3.3 Peak of the T Wave

The T wave succeeds the QRS complex. The amplitude of its peak differs considerably from the baseline, however no general statement can be given about its absolute values or the amplitude relative to the R peak. Also, its polarity depends on the location of measurement of the ECG signal [4]. Therefore, a function detecting peaks independently of their polarity has to be used for the detection of the peak of the T wave.

A special “wings” function  $W$ , described by Christov and Simova [9], is used to detect the peak of the T wave. It is calculated as follows ( $w = 40$  ms):

$$W1_t = T_{t-w} - T_t \quad (15)$$

$$W2_t = T_t - T_{t+w} \quad (16)$$

$$W_t = W1_t \cdot W2_t. \quad (17)$$

This “wings” function is calculated for the Template  $T_t$  in the interval between the last QRS offset and the end of the template. As shown in Figure 5, the minimum of the “wings” function corresponds to the peak of the T wave, regardless of the polarity of the T wave. Therefore, the point of the minimum of the “wings” function is used as reference for the detection of the T wave’s peak. Subsequently, the exact position of the peak is determined on the original signal by finding the next local minimum or maximum, depending on the T wave’s polarity.



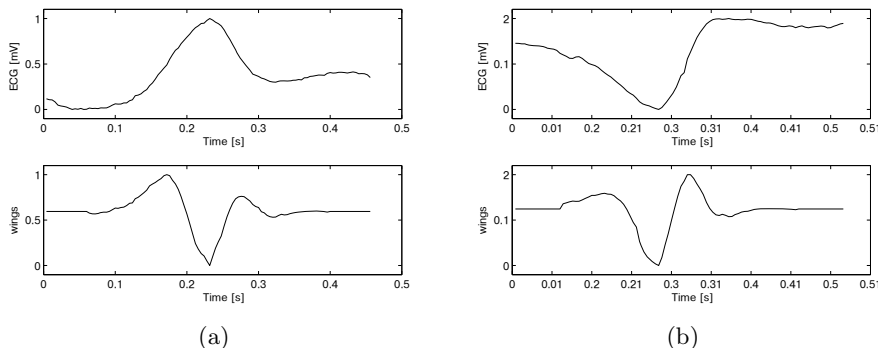


**Fig. 5.** Top: differently shaped T waves ((a) positive T wave, (b) negative T wave). Bottom: Corresponding “wings” function.

### 3.4 On- and Offset of the T Wave

The onset of the T wave precedes the peak of the T wave and is located in the area where the amplitude of the signal approaches the baseline or its slope flattens. The offset succeeds the peak of the T wave in the same way. Since there is no guarantee that the signal’s value or first derivative reach certain thresholds, a geometric method is utilised for the detection of these points.

Figure 6 illustrates the geometric method used to detect the onset of the T wave. It is calculated as follows:

- Determine the straight line  $g_t$  connecting the QRS offset and the peak of the T wave of the signal  $S_t$ :

$$k = \frac{S_{T\_peak} - S_{QRS\_offset}}{T\_peak - QRS\_offset} \quad (18)$$

$$d = S_{QRS\_offset} - k \cdot QRS\_offset \quad (19)$$

$$g_t = k \cdot t + d. \quad (20)$$

- Subtract  $g_t$  from the signal  $S_t$ :

$$S_t^* = S_t - g_t. \quad (21)$$

- The minimum of  $S_t^*$  is annotated as the onset of the T wave.

The offset of the T wave is determined in the same way by using a straight line between the peak of the T wave and the end of the template.

### 3.5 P Wave

The P wave precedes the QRS complex and is very similar to the T wave, therefore it can be analysed using similar methods. In contrast to the P wave, it can only have positive polarity and its amplitude is usually very low.

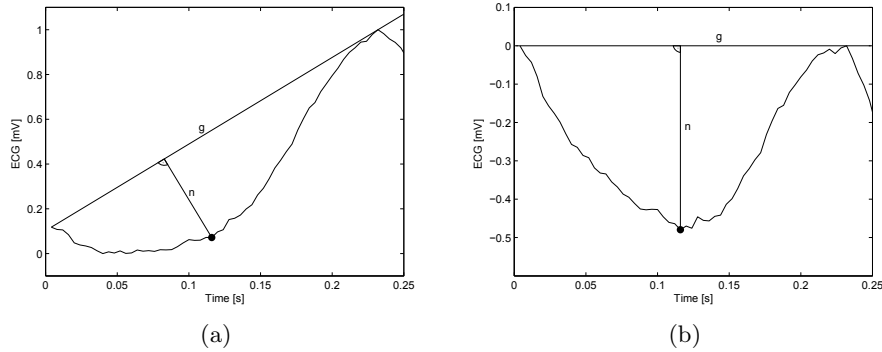


**Fig. 6.** Geometric method to determine the onset of the T wave. (a) Connecting the QRS offset and the peak of the T wave by the straight line  $g$ . Finding the longest line  $n$  intersecting  $g$  and the signal with a right angle between  $g$  and  $n$ . (b) Simplification of the calculation by subtraction of  $g$  from the signal. The intersection of  $n$  with the signal corresponds to the minimum of the signal.

The interval between the previous offset of the T wave and the current onset of the QRS complex is analysed on the template to detect the peak of the P wave. A slightly altered version of the “wings” function (equations 15, 16, and 17), which only reacts to positive waves, is used for this analysis. Onset and offset of the P wave are detected with the same method as on- and offset of the T wave.

#### 4 Differences between Online and Offline Algorithm

Both, the online and the offline version of the algorithm, follow the steps described in the previous section. The only differences are the order of the classification, the calculation of the template for the detected classes, and the available memory.

The online version of the algorithm has no information about future signal values, therefore the classification is performed every time an R peak is detected. Also, the template is rebuilt whenever a class receives new information, thus after each new R peak. Hence, in the beginning of the measurement, the online algorithm has very little information about possible different waveforms to be analysed. In the first few seconds, the template is built based on only a few heartbeats and therefore cannot develop its full capabilities of signal smoothing and noise reduction. As the measurement continues the online version of the algorithm receives more information and produces better results.

The offline version of the algorithm on the other hand is able to analyse the whole signal at once. It classifies all detected heartbeats prior further investigation and is thus able to build the template from all available information. Therefore, the quality of the annotations stays constant throughout the whole measurement.

Considering the memory available for the analysis, the offline version of the algorithm has the advantage of being carried out on an ordinary personal computer. It can receive an arbitrary amount of memory and can access all values of the signal at any time. Contrary, the online version of the algorithm is designed to be used on an embedded system with very limited amount of memory. The online algorithm hence will not store all signal values in the memory, but only the templates of the classes based on previously detected heartbeats. Thus, the memory needed depends only on the numbers of classes that are to be distinguished. Since this value is predefined, the amount of memory needed by the online version of the algorithm can be predicted and adapted to the resources of the embedded system.

## 5 Results

The verification of the results of the algorithm was performed by comparing them to the results of medical experts. The PhysioNet databases provide recordings of different physiological modalities and corresponding annotations by medical experts, hence these databases are an ideal data source for the verification [15,16].

Due to the different original purpose of these databases, the amount and quality of these annotations varies. After assessing the signals and the annotations, the following four databases were chosen for the verification:

- QT Database, created to evaluate algorithms detecting the QT interval [18].
- AF Termination Challenge Database, designed to be used in the “Computers in Cardiology Challenge 2004” [19].
- MIT-BIH Arrhythmia Database, test material for evaluation of arrhythmia detectors [20].
- Fantasia Database, originally used for testing automated arrhythmia detection [21].

All four databases were used in the assessment of the detection rate of R peaks of the algorithm. The following two parameters are recommended by the American National Standards Institute (ANSI) for the evaluation of the detection rate [22]:

- The sensitivity  $Se$

$$Se = \frac{TP}{TP + FN} \quad (22)$$

- and the positive predictive value  $PPV$

$$PPV = \frac{TP}{TP + FP}, \quad (23)$$

where  $TP$  is the number of true positive,  $FN$  the number of false negative and  $FP$  the number of false positive detections.

**Table 1.** Means and standard deviations of differences in time between annotated and detected points as well as between different expert annotations. “Online” refers to the features detected by the online version of the algorithm executed on the embedded system in real time, whereas “Offline” refers to the offline version of the algorithm executed on a PC.

Feature	Online vs. Experts		Offline vs. Expert		Inter-expert diff.	
	$\mu$	$\sigma$	$\mu$	$\sigma$	$\mu$	$\sigma$
P Onset	1.9 ms	19.0 ms	1.2 ms	19.2 ms	*	*
P Peak	0.2 ms	16.1 ms	0 ms	10.3 ms	*	*
P Offset	-0.9 ms	17.9 ms	-0.2 ms	14.1 ms	*	*
QRS Onset	0.5 ms	10.2 ms	-2.2 ms	10.3 ms	3.8 ms	14.2 ms
R Peak	-9.1 ms	14.3 ms	-9.4 ms	14.4 ms	0.1 ms	2.4 ms
QRS Offset	4.3 ms	12.6 ms	8.3 ms	13.6 ms	2.7 ms	17.0 ms
T Onset	24.9 ms	43.4 ms	4.4 ms	45.4 ms	9.5 ms	44.9 ms
T Peak	-3.4 ms	32.9 ms	-1.7 ms	33.9 ms	3.5 ms	30.0 ms
T Offset	-4.0 ms	38.7 ms	0.3 ms	40.4 ms	5.8 ms	39.9 ms

\* Annotated by one expert only

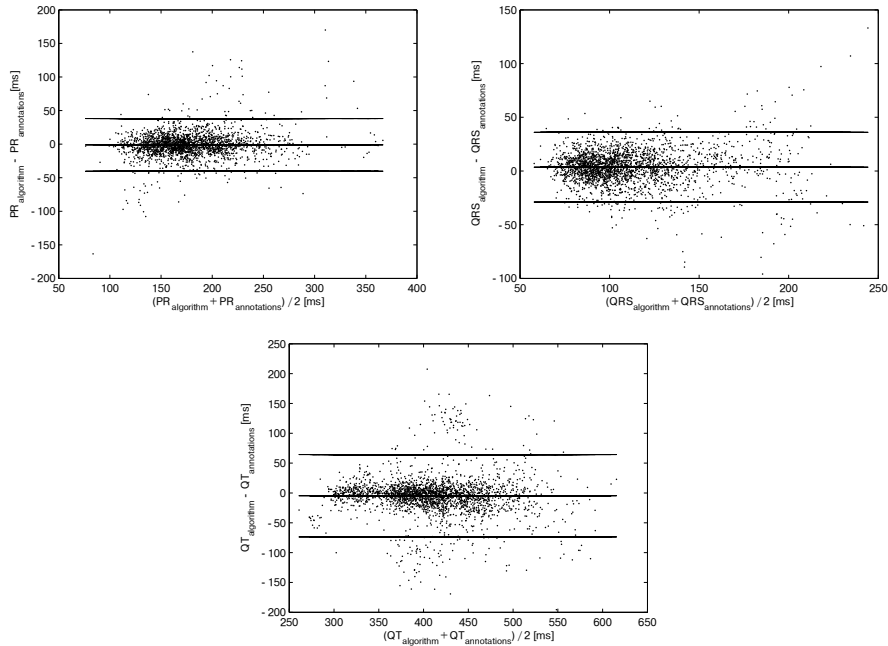


**Fig. 7.** Bland-Altman diagrams showing the differences between results of the algorithm and results of medical experts

A sensitivity of 98.2% and a positive predictive value of 98.7% were achieved in the verification of the detection rate by the offline as well as the online version of the algorithm.

On- and offset of the QRS complex and P and T wave were only annotated by medical experts in the QT database. Hence, this was the only database used for the verification of these features. The time differences between detected and corresponding annotated points are shown in Table 1.

Finally, the durations of the QT and the PR intervals and the QRS complexes were calculated from the results of the algorithm and the expert annotations, respectively. Figure 7 shows Bland-Altman diagrams comparing the results of the algorithm with those of the medical experts [23]. Means and standard deviations of the differences are  $-1.1 \pm 10.0$  ms for the PR interval,  $3.6 \pm 16.5$  ms for the QRS complex and  $-4.7 \pm 35.2$  ms for the QT interval. These results are satisfying and match existing offline algorithms [7,8,24].

## 6 Discussion and Conclusion

The majority of the means of differences found in Table 1 are smaller than the sampling interval of 4 ms, suggesting an insignificant error. The standard deviations of the differences between the results of the medical experts and the algorithm are also very similar to those of inter-expert differences. As they reflect the uncertainty in the annotation of the features among experts, these results suggest that the algorithm performs approximately as well as humans.

Two outliers can be identified in Table 1: The R peak and the T onset. These findings can be traced back to unusual annotations in the QT Database. Sometimes, negative peaks within the QRS complex are marked as R peaks, whereas they ought to be positive by definition. Due to the occasional overlapping of T waves with QRS complexes the exact position of the onset of the T wave can be ambiguous. The comparatively high standard deviation of the inter-expert differences also reflects this fact.

The detection rates of the offline and the online version of the algorithm are identical as both versions use the same detection strategy for R peaks. However, comparing their accuracy as shown in Table 1, the offline algorithm achieves slightly better results. This outcome was to be expected due to the fact that the offline algorithm is able to analyse the whole signal at once whereas the online algorithm has no information about future signal values.

In the analysis of the Bland-Altman diagrams in Figure 7 no trends or shifts can be found, therefore not suggesting any methodical error. Their means are in the range of the sampling interval and therefore indicate only a minimal error. Since the standard deviations are in the same range as those in Table 1, they show no abnormalities.

## 7 Future Work

The algorithm presented in this paper only works on one ECG signal, thus the next step of the development will be an extension to several ECG leads. This enhancement will allow for a better detection of motion artefacts or even a continuous analysis despite incomplete data. Therefore, the enhanced algorithm

can be used on data from 24 hour ECG measurements. This will allow the evaluation of the heart rate variability (HRV) and dynamic changes in all other detected features and intervals as well as the analysis of the approximate entropy of ECG signals [25].

**Acknowledgements.** This work was partly supported by a grant of the Government of Lower Austria and the EC (EFRE), contract number WST3-T-81/015-2008.

## References

1. Allender, S., Scarborough, P., Peto, V., Rayner, M., Leal, J., Luengo-Fernandez, R., Gray, A.: European cardiovascular disease statistics. Brussels: European Heart Network (2008)
2. Roger, V.L., Go, A.S., Lloyd-Jones, D.M., Adams, R.J., Berry, J.D., Brown, T.M., Carnethon, M.R., Dai, S., de Simone, G., Ford, E.S., et al.: Heart disease and stroke statistics–2011 update: A report from the american heart association. *Circulation* 123(4), e18–e209 (2011)
3. Rangayyan, R.M.: *Biomedical Signal Analysis: A Case-Study Approach*. IEEE Press (2002)
4. Luthra, A.: *ECG made easy*. Jaypee Brothers Medical Pub. (2012)
5. U.S. Department of Health and Human Services - Food and Drug Administration and Center for Drug Evaluation and Research (CDER) and Center for Biologics Evaluation and Research (CBER). Guidance for industry: E14 clinical evaluation of qt/qt<sub>c</sub> interval prolongation and proarrhythmic potential for non-antiarrhythmic drugs. Regulatory Information (October 2005)
6. Chouhan, V.S., Mehta, S.S.: Detection of qrs complexes in 12-lead ecg using adaptive quantized threshold. *IJCSNS* 8(1), 155 (2008)
7. Köhler, B.U., Hennig, C., Orglmeister, R.: The principles of software qrs detection. *IEEE Engineering in Medicine and Biology Magazine* 21(1), 42–57 (2002)
8. Hayn, D., Kollmann, A., Schreier, G.: Automated qt interval measurement from multilead ecg signals. In: *Computers in Cardiology*, pp. 381–384. IEEE (2008)
9. Christov, I., Simova, I.: Fully automated method for QT interval measurement in ECG. In: *Computers in Cardiology*, pp. 321–324. IEEE (2006)
10. Diery, A., Rowlands, D., Cutmore, T.R.H., James, D.: Automated ecg diagnostic p-wave analysis using wavelets. *Computer Methods and Programs in Biomedicine* (2010) (in Press, Corrected Proof)
11. Holzinger, A., Scherer, R., Seeber, M., Wagner, J., Müller-Putz, G.: Computational Sensemaking on Examples of Knowledge Discovery from Neuroscience Data: Towards Enhancing Stroke Rehabilitation. In: Böhm, C., Khuri, S., Lhotská, L., Renda, M.E. (eds.) *ITBAM 2012. LNCS*, vol. 7451, pp. 166–168. Springer, Heidelberg (2012)
12. Bachler, M., Hametner, B., Mayer, C., Kropf, J., Gira, M., Wassertheurer, S.: Automated verification of cardiovascular models with continuous integration tools. In: Breitenecker, F., Bruzzzone, A., Jimenez, E., Longo, F., Merkurjev, Y., Sokolov, B. (eds.) *The 24th European Modeling & Simulation Symposium*, pp. 316–321. DIME Università di Genova (September 2012)
13. Berg, A.: *Jenkins Continuous Integration Cookbook*. Packt (2012)

14. Duvall, P., Matyas, S., Glover, A.: Continuous integration: improving software quality and reducing risk. Addison-Wesley Professional (2007)
15. Goldberger, A.L., Amaral, L.A.N., Glass, L., Hausdorff, J.M., Ivanov, P.C., Mark, R.G., Mietus, J.E., Moody, G.B., Peng, C.-K., Stanley, H.E.: Physiobank, physiotoolkit, and physionet: Components of a new research resource for complex physiologic signals. *Circulation* 101(23), e215–e220 (2000), *Circulation Electronic Pages*, <http://circ.ahajournals.org/cgi/content/full/101/23/e215>
16. PhysioNet, Physiobank, <http://physionet.org/physiobank/database/>
17. Iaizzo, P.A.: Handbook of Cardiac Anatomy, Physiology, and Devices. Humana Press, a part of Springer Science+ Business Media, LLC, Totowa, NJ (2009)
18. Laguna, P., Mark, R.G., Goldberg, A., Moody, G.B.: A database for evaluation of algorithms for measurement of qt and other waveform intervals in the ecg. In: *Computers in Cardiology 1997*, pp. 673–676 (1997)
19. PhysioNet and Computers in Cardiology. Spontaneous termination of atrial fibrillation - a challenge from physionet and computers in cardiology (2004), <http://www.physionet.org/challenge/2004/>
20. Moody, G.B., Mark, R.G.: The impact of the mit-bih arrhythmia database. *IEEE Engineering in Medicine and Biology Magazine* 20(3), 45–50 (2001)
21. Iyengar, N., Peng, C.K., Morin, R., Goldberger, A.L., Lipsitz, L.A.: Age-related alterations in the fractal scaling of cardiac interbeat interval dynamics. *American Journal of Physiology-Regulatory, Integrative and Comparative Physiology* 271(4), R1078–R1084 (1996)
22. Ansi/aami ec57: Testing and reporting performance results of cardiac rhythm and st segment measurement algorithms (October 1998), <http://www.aami.org>, Order Code: EC57-293
23. Bland, J.M., Altman, D.G.: Statistical methods for assessing agreement between two methods of clinical measurement. *The LANCET* 1, 307–310 (1986)
24. Schreier, G., Hayn, D., Lobodzinski, S.: Development of a new qt algorithm with heterogenous ecg databases. *Journal of electrocardiology* 36, 145–150 (2003)
25. Holzinger, A., Stocker, C., Bruschi, M., Auinger, A., Silva, H., Gamboa, H., Fred, A.: On Applying Approximate Entropy to ECG Signals for Knowledge Discovery on the Example of Big Sensor Data. In: Huang, R., Ghorbani, A.A., Pasi, G., Yamaguchi, T., Yen, N.Y., Jin, B. (eds.) *AMT 2012. LNCS*, vol. 7669, pp. 646–657. Springer, Heidelberg (2012)